ACS chemical biology

Articles

pubs.acs.org/acschemicalbiology

Terms of Use

Membrane Environment Can Enhance the Interaction of Glycan Binding Protein to Cell Surface Glycan Receptors

Lei Shen,[†,∥] Yini Wang,[‡] Chia-I Lin,[§] Hung-wen Liu,*[,§] Athena Guo,*[,‡] and X.-Y. Zhu*[,†]

[†]Department of Chemistry, Columbia University, New York, New York 10027, United States

[‡]Microsurfaces, Inc., 1 West Forest Avenue, Englewood, New Jersey 07631, United States

[§]College of Pharmacy, University of Texas at Austin, Austin, Texas 78712, United States

Supporting Information

ABSTRACT: The binding of lectins to glycan receptors on the host cell surface is a key step contributing to the virulence and species specificity of most viruses. This is exemplified by the viral protein hemagglutinin (HA) of the influenza A virus, whose binding specificity is modulated by the linkage pattern of terminal sialic acids on glycan receptors of host epithelial cells. Such specificity dictates whether transmission is confined to a particular animal species or jumps between species. Here, we show, using H5N1 avian influenza as a model, that the specific binding of recombinant HA to α2-3 linked sialic acids can be enhanced dramatically by interaction with the surface of the lipid membrane. This effect can be quantitatively accounted for by a two-stage process in which weak association of HA with the membrane surface precedes more specific and tighter binding to the glycan receptor. The weak protein−membrane interaction discovered here in the model system may play an important secondary role in the infection and pathogenesis of the influenza A virus.

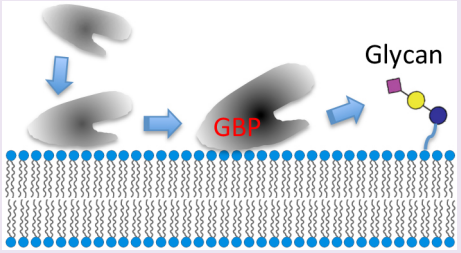

Pathogen recognition and attachment onto host cells often starts with the binding of glycan binding proteins (GBPs) to glycan receptors on the host cell surface.[1] Here, we probe this initial binding event using a model system related to the influenza A virus. One of the most important questions in influenza research is how a new strain of influenza A virus may emerge to cause human outbreak or pandemic. Unfortunately, there is still no clear answer today, and this has led to the intense research interest and public anxiety on the subject.[2,3] The demonstrations of genetically altered H5N1 strains to more readily infect mammalian species,[4−6] and the recent outbreaks in human populations of the H1N1 swine virus[7] and the H7N9 avian virus,[8] all underscore the urgency in finding answers to this question. Past studies of the transmission of influenza A viruses have focused on the specificity of the viral transmembrane protein hemagglutinin (HA) for glycan receptors on host cell surfaces.[9,10] These glycan receptors contain sialic acid, also known as N-acetylneuraminic acid (Neu5Ac), and vary in structure from hosts to hosts. HA exists as trimers in the viral membrane and the weak interaction between each HA and its glycan receptor[11] is strengthened by multivalent binding to each HA trimer and to multiple trimers on the virus surface.[12] The HA proteins of human-adapted influenza A bind preferentially to α2-6 linked sialic acid, whereas those of avian-adapted strains are more specific for α2-3 linked sialic acid, Scheme 1.[13−17] There is also significant cross reactivity, which depends on the chemical nature of the glycan backbones and functional group modification of the sugar components.[14−16] Recent studies suggested two general topologies of these glycans with respect to their specificities;

Scheme 1. Schematic Illustration of Oligo-glycans with α2-6 and α2-3 Terminal Linkage to Sialic Acid

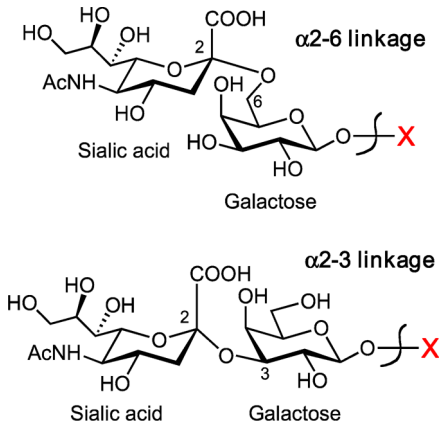

HAs with high-affinity to human-adapted influenza A viruses are characterized by a broad "umbrella-like" topology while those for avian-adapted ones adopt a narrower "cone-like" topology.[16,18]

The binding of glycan binding protein (GBP) molecules on a virus to glycan receptors on the host cell surface is unlikely a direct and single step, particularly when multivalency is involved. Rather, the binding event is expected to be a dynamic

Received: February 25, 2014
Accepted: June 20, 2014
Published: June 20, 2014

Scheme 2. Structures of Glycolipids and Other Functionalized Lipids Used in the Present Study[a]

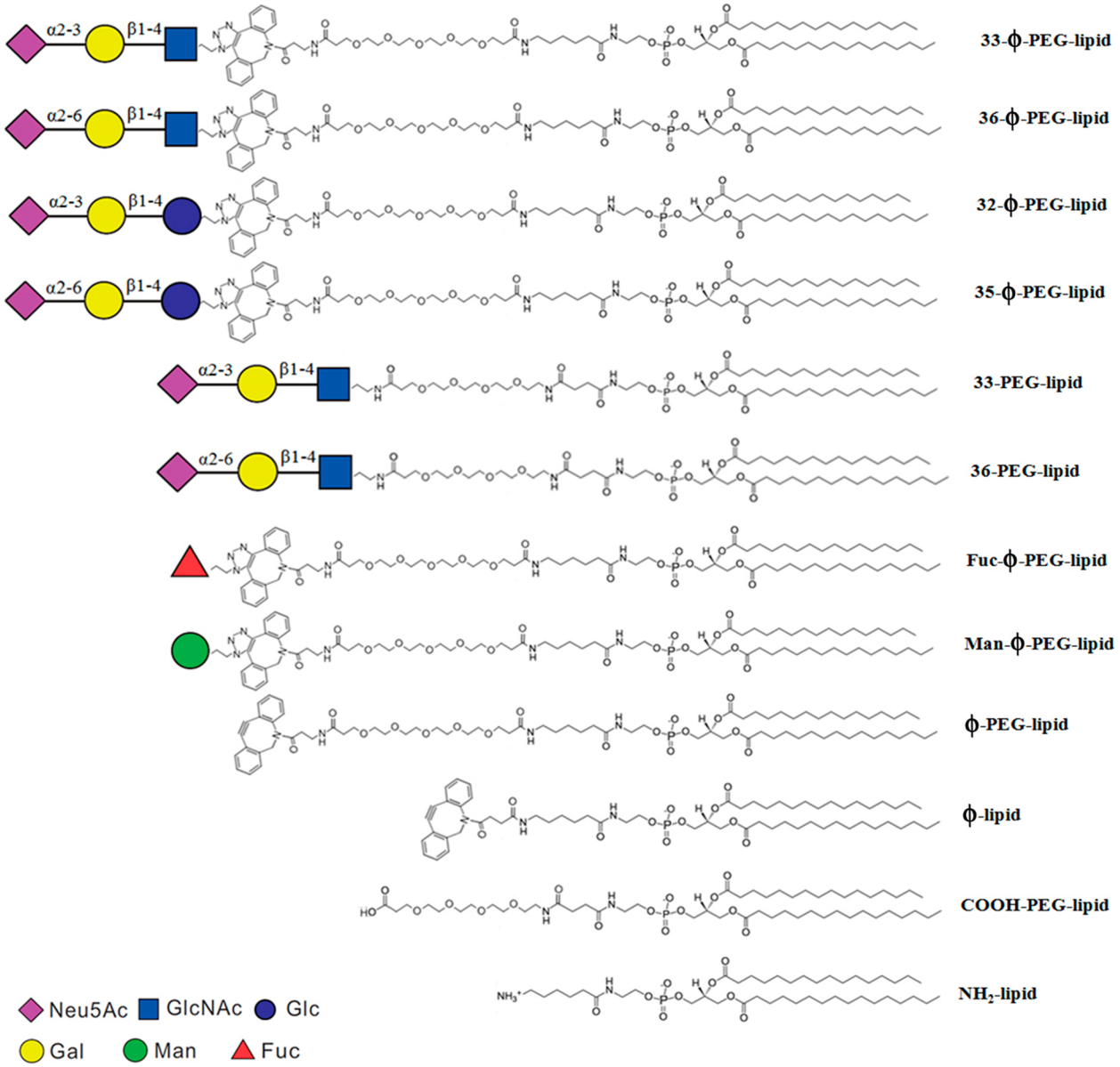

[a] ϕ refers to the hydrophobic dibenzocyclooctyne group for linking azido-functionalized sugar molecules to the lipid anchors using Cu-free click chemistry. The colored symbols represent sugar groups. Neu5Ac: N-acetylneuraminic acid. GlcNAc: N-acetylated glucose. Glc: glucose. Man: mannose. Fuc: fucose. Gal: galactose.

process involving intermediates before the multiple GBP-glycan receptor interaction partners are established. Evidences suggesting the formation of weakly bound intermediates in interfacial interactions can be found in a wide range of chemical and biological processes. For example, the involvement of weakly bound species called "precursors" is believed to play essential roles in the adsorption of small molecules,[19] polymers,[20,21] and proteins[22,23] at interfaces. In the formation of protein−protein complex, the process is believed to begin with a solvated encounter complex, followed by one or more weakly bound intermediate states before the final complex is formed.[24] Zhu et al. demonstrated a similar precursor mechanism in the adhesion of a bacteria cell, *Escherichia coli* (*E. coli*), to mannose receptors on model lipid membrane surfaces: *E. coli* cells can adhere to the membrane surface in both a weakly bound, monovalent state and a strongly bound, multivalent one.[25]

In the case of GBP-glycan complex formation, the surfaces of both the virus and the host cell are highly heterogeneous, with the binding partners embedded in complex and dynamic environments.[9,10] We hypothesize that formation of the specific GBP-glycan complex is also preceded by weakly bound precursors that are sensitive to the local physicochemical environment on the cell membrane surface. As a first step toward understanding the mechanism by which the GBP-glycan complexes are formed, we have investigated the binding kinetics of recombinant HA from the H5N1 avian influenza A virus to specific glycan receptors on model cell membrane surfaces. For this purpose, we have used label-free fluidic glycan microarrays. While microarrays of immobilized glycans have been successfully used before for the determination of binding

dx.doi.org/10.1021/cb5004114 | ACS Chem. Biol. 2014, 9, 1877−1884

specificity of HAs from various influenza A virus sources,[14,17] we prefer microarrays of glycans (glycolipids) in the fluidic supported lipid bilayer (SLB) environment to better mimic the dynamic environment of cell membrane.[25] We combined the SLB microarray with surface plasmon resonance (SPR) imaging for label-free and real-time measurement of binding kinetics. SPR has been applied in the past to determine HA binding kinetics with glycan receptors, but not in the array format.[26−28]

The fluidic SLB format allowed us to easily tune the composition of the model membrane surface by quantitatively mixing functional lipids with matrix lipids for SLB formation. We systematically tuned the environment for HA-glycan complexes and show that the HA-glycan receptor binding rate can be enhanced many folds by changes to the lipid membrane surface, an effect that can be quantitatively accounted for by a precursor-mediated mechanism. We suggest that such a precursor mechanism is of general importance to GBP/glycan receptor interaction on cell membranes.

RESULTS AND DISCUSSION

The model system we choose is recombinant HA protein[12] from the highly pathogenic H5N1 A/Vietnam/1203/2004 (Viet04).[29] In solution, the recombinant HA proteins are known to be present mostly in the trimeric form as on the virus surface, with a distribution of oligomeric structures.[30,31] Glycan receptors were prepared as glyco-lipids and incorporated into supported lipid bilayer (SLB), which serve to mimic the cell membrane.[32] We adjusted the chemical environment on the membrane surface by incorporating functionalized lipid molecules in a matrix of egg phosphatidylcholine (eggPC). We fabricated the SLB in an array format[33,34] on a gold sensor surface for label-free detection via surface plasmon resonance (SPR) imaging, as detailed in Supporting Information (Figure S1). The fluidic nature of the SLB on the array was verified by fluorescence recovery after photobleaching (FRAP), as shown in Supporting Information Figure S2. The spots on each array contain different concentrations of glyco- and functional lipids in the eggPC matrix. We obtained parallel binding kinetics of HA to all spots on the array by recording SPR images (SPRImager II, GWC Technologies Inc., Madison, WI) as a function of time.

The structures of all glycolipids and other functionalized lipids used in the present study are shown in Scheme 2. Trisaccharides possessing α2-3 linked sialic acid are represented by Neu5Ac-α2-3-Gal-β1-4-GlcNAc (**33**) and Neu5Ac-α2-3-Gal-β1-4-Glc (**32**). These glycolipids are designed to specifically bind HA from avian H5N1. In contrast, trisaccharides possessing α2-6 linked sialic acid are represented by Neu5Ac-α2-6-Gal-β1-4-GlcNAc (**36**) and Neu5Ac-α2-6-Gal-β1-4-Glc (**35**), and are designed to bind HA from human-adapted influenza A. The sialic acid residues in both sets of trisaccharides contain terminal azide ($-N_3$) functional groups and were obtained from the Consortium for Functional Glycomics.[35] These trisaccharides were conjugated to one of the two lipid anchors, 16:0 Caproylamine PE, which is short for 1,2-dipalmitoyl-*sn*-glycero-3-phosphoethanolamine-N-(hexanoylamine), or 16:0 succinyl PE, which is short for 1,2-dipalmitoyl-*sn*-glycero-3-phosphoethanolamine-N-(succinyl) (Avanti Polar Lipids, Alabaster, AL). The conjugation was done via oligo(ethylene glycol) (OEG) linkers either through Cu-free click chemistry with a dibenzocyclooctyne (ϕ) group,[36] or through an *N*-hydroxysuccinimide (NHS) coupling reaction to the amine functionality generated by reducing the azides. To change the membrane environments, we used six different functionalities anchored to lipids: the hydrophilic mannose or fucose linked to OEG-lipid via Cu-free click chemistry (**Man**-ϕ-OEG-lipid or **Fuc**-ϕ-OEG-lipid), the hydrophobic cyclooctyne group conjugated with or without OEG linker to the lipid molecule (ϕ-OEG-lipid or ϕ-lipid), and the acidic $-$COOH or basic $-NH_2$ terminated lipids (**HOOC**-OEG-lipid or **H_2N**-lipid). The synthesis and characterization of these lipid molecules are detailed in Supporting Information.

We incorporated each of the above glycolipids and the functionalized lipids into the SLB microarray and measured the binding of the recombinant HA protein using SPR. In the experiment, the microarray surface was first equilibrated with the buffer solution, followed by the injection of HA protein solution (marked by a downward arrow) and, after some time, the injection of washing buffer to remove the unbound HA (upward arrow).

We first established the specificity of HA binding to glycan receptors on the model cell membrane. Figure 1A shows typical SPR kinetic profiles for the trisaccharides (in eggPC matrix). Consistent with the known specificity of the avian H5N1 HA protein, binding was only observed to the α2-3 linked sialic acids (**33**-ϕ-OEG-lipid, **33**-OEG-lipid, and **32**-ϕ-OEG-lipid, solid curves), with no detectable binding to α2-6 linked trisaccharides (**36**-ϕ-OEG-lipid, **36**-OEG-lipid, and **35**-ϕ-OEG-

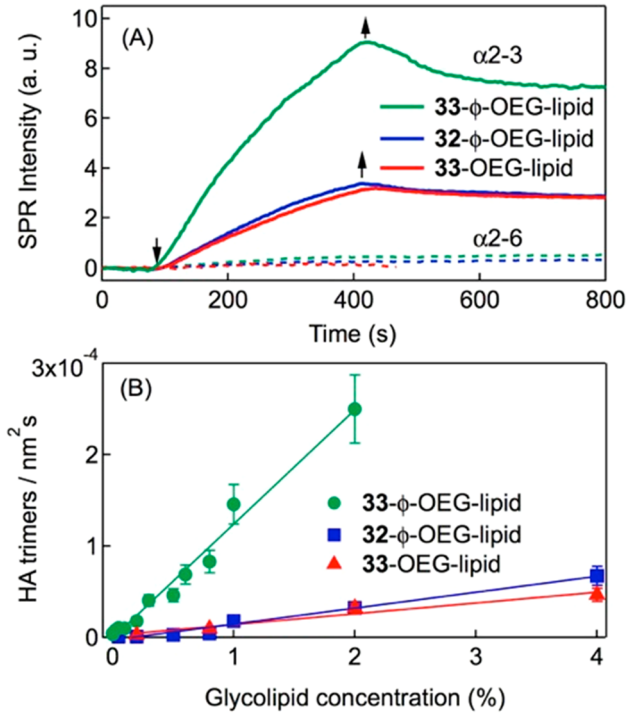

Figure 1. (A) SPR responses for the binding of recombinant HA protein (400 nM) with α2-3 linked sialic acids (solid curves: green, **33**-ϕ-OEG-lipid; blue, **32**-ϕ-OEG-lipid; red, **33**-OEG-lipid) and with α2-6 linked sialic acids (dashed curves: green, **35**-ϕ-OEG-lipid; red, **36**-ϕ-OEG-lipid; blue, **36**-PEG-lipid) on a supported lipid bilayer microarray. The density of **33**-ϕ-OEG-lipid is 0.8% and those of all others are 4.0%. The downward and upward arrows indicate the times of protein solution and washing buffer injections, respectively. (B) The initial association rates of HA trimers (nm^{-2} s^{-1}) as a function of the specific glycolipid concentration in the SLB. The symbols are data points and solid lines are linear fits. Green, **33**-ϕ-OEG-lipid; blue, **32**-ϕ-OEG-lipid; and red, **33**-OEG-lipid.

dx.doi.org/10.1021/cb5004114 | ACS Chem. Biol. 2014, 9, 1877−1884

lipid, dashed curves). Furthermore, no measurable binding of HA to any other functionalized lipids was observed (Supporting Information Figure S3). For the three α2-3 trisaccharides, we found that the initial rate of HA binding is proportional to the concentration of glycolipid in the SLB, Figure 1B, as expected from the initial binding kinetics at low surface HA coverage (see kinetic analysis below). For the three glycolipids containing α2-3 linked sialic acid, the association rate of HA with **33**-ϕ-OEG-lipid is approximately 4× that with either **33**-OEG-lipid or **32**-ϕ-OEG-lipid. Here, **33**-ϕ-OEG-lipid and **33**-OEG-lipid possess the same trisaccharide and differ only in the linkage: the bulkier click-linkage (ϕ) to OEG in the former or the peptide linkage to OEG in the latter. The hydrophobic ϕ linking group may increase secondary interaction with hydrophobic domains near the HA binding site,[37] leading to enhanced interaction with the glycan receptor (**33**).For **33**-ϕ-OEG-lipid and **32**-ϕ-OEG-lipid, the difference is only in the third sugar unit. The sensitivity of HA-glycan complex formation to interactions beyond the linkage pattern of the terminal sialic acid has been observed before.[12,16] Note that, for simplicity, we use the density of trimers in the data analysis, as they are the predominant species from recombinant HA. The actual surface HA species are likely a distribution of oligomers,[30,31] but the conclusions remain unchanged.

We now turn to the focus of this study: the investigation of the influence that membrane environment has on HA−glycan complex formation. In this experiment, we used a fixed concentration (0.8%) of **33**-ϕ-OEG-lipid in the membranes in the presence of a second functionalized lipid with a variable concentration (0−4%). None of these secondary lipids alone (in eggPC matrix) showed any binding to HA (see Supporting Information Figure S3). Figure 2A shows SPR responses for HA binding to **33**-ϕ-OEG-lipid with the hydrophobic ϕ-OEG-lipid as the secondary functionalized lipid. The addition of ϕ-OEG-lipid dramatically increases the rate of HA binding to **33**-ϕ-OEG-lipid, by as much as 4× when the ϕ-OEG-lipid concentration in the SLB is increased from 0 to 4%. Since ϕ-OEG-lipid alone shows no measurable affinity to HA (Supporting Information Figure S3), we conclude that its effect in the lipid membrane is to assist the binding of HA to **33**-ϕ-OEG-lipid. An important feature of this assistance effect is that the addition of ϕ-OEG-lipid leads to a systematic increase in the rate of association between HA and **33**-ϕ-OEG-lipid, but little change to the rate of dissociation of HA-**33**-ϕ-OEG-lipid complex. In addition, the association parts of all the SPR profiles, that is, integrated rate equations (concentration vs time) are superimposable with different multiplication factors (Supporting Information Figure S4).

Similar results were obtained with other secondary functionalized lipids that showed lesser extents of enhancement or inhibition of HA binding with **33**-ϕ-OEG-lipid, as detailed later in Figure 4. For example, Figure 2B shows SPR responses for HA binding to **33**-ϕ-OEG-lipid with the hydrophilic $\mathbf{H_2N}$-OEG-lipid as the secondary lipid. Within experimental uncertainty, the addition of $\mathbf{H_2N}$-OEG-lipid to the eggPC matrix has no effect on either the association or dissociation of HA with **33**-ϕ-OEG-lipid. Another interesting comparison to make would be **33**-ϕ-OEG-lipid versus **33**-ϕ-lipid; unfortunately, we were not able to carry out the click reaction between **33**-azide and ϕ-lipid due to mismatch in solubility between these two molecules.

The observed dependence of complex formation between HA and **33**-ϕ-OEG-lipid on the nature of the membrane

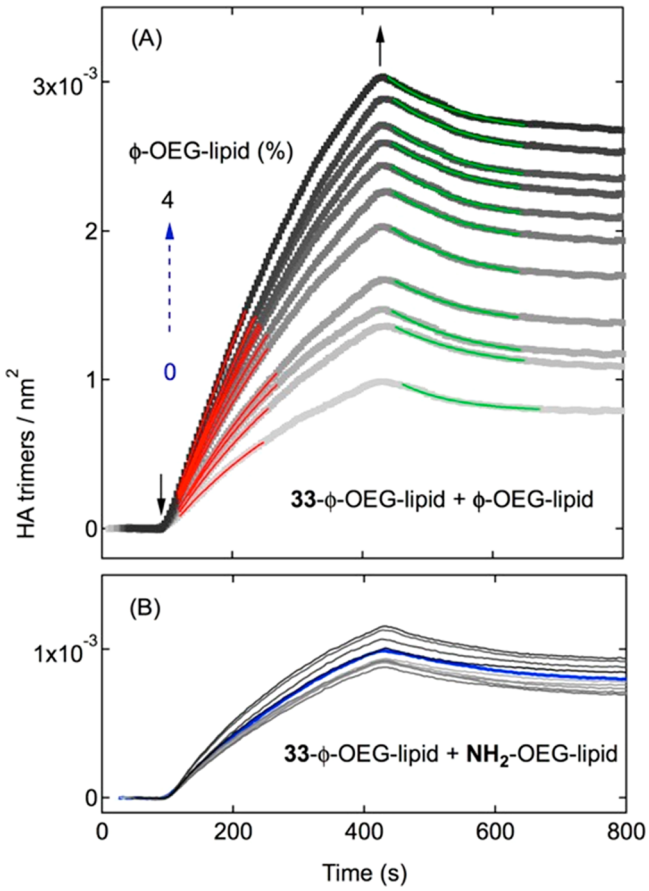

Figure 2. SPR responses for the interaction of HA protein (0.4 μM) with glycolipids on an SLB array. In each spot (curve), the concentration of α2-3 linked sialic acid **33**-ϕ-OEG-lipid is kept constant (0.8 mol %), while the concentration of the second lipid molecule (A, ϕ-OEG-lipid; B, $\mathbf{H_2N}$-OEG-lipid) is varied from 0% to 0.05, 0.1, 0.3, 0.5, 0.8, 1.0, 1.5, 2.0, 3.0, and 4.0 mol %. In panel A, the concentrations of ϕ-OEG-lipid (0−4%) are represented by gray scale with increasing darkness. The red curves are fits to eq 3 and the green curves to eq 6. In panel B, the 0% $\mathbf{H_2N}$-OEG-lipid concentration is represented by the blue curve, with all other concentrations as gray curves.

surface environment contradicts the commonly used (but incorrect) model of direct binding of a solution phase protein molecule to glycan receptors on the membrane surface, as the influence of the membrane environment on the kinetics of complex formation is ignored in such a model. Rather, the kinetic results in Figure 2 can be satisfactorily and *quantitatively* explained by a precursor mechanism. In the simplest form, the precursor mechanism can be represented by

$$\text{(i) } P \underset{k_{-1}}{\overset{k_1}{\rightleftharpoons}} P^* \qquad \text{(ii) } P^* + \underline{G} \underset{k_{-2}}{\overset{k_2}{\rightleftharpoons}} \underline{PG}$$

$$\text{(iii) } \underline{PG} + \underline{G} \underset{k_{-3}}{\overset{k_3}{\rightleftharpoons}} \underline{PG_2} \quad \text{(iv) } \underline{PG_2} + \underline{G} \underset{k_{-4}}{\overset{k_4}{\rightleftharpoons}} \underline{PG_3} \qquad (1)$$

where P is HA protein (trimer) free in solution; P^* represents the precursor state, that is, protein molecules transiently adsorbed on the membrane surface before specific binding to the glycan receptor ($\underline{G}$) to form bound protein-glycan complexes ($\underline{PG_x}$). The HA trimer can bind up to three glycan receptors,[12] as shown by steps (iii) and (iv) in eq 1, but the SPR technique only measures the total amount of protein

dx.doi.org/10.1021/cb5004114 | ACS Chem. Biol. 2014, 9, 1877−1884

Table 1. Kinetic Parameters for HA Binding to 33-ϕ-OEG-Lipid in the Supported Lipid Bilayer with Different Concentrations of ϕ-OEG-Lipid[a]

ϕ-OEG-lipid (%)	α (nm^{-2})	β (s^{-1})	$\beta_d = k_d$ (s^{-1})	k_a (s^{-1} M^{-1})	K_D (μM)	$[\underline{PG_x}]_0$ (nm^{-2})	$[\underline{PG}]_0$ (nm^{-2})
0	1.3×10^{-3}	4.0×10^{-3}	1.0×10^{-2}	1.0×10^{4}	1.0	7.8×10^{-4}	2.0×10^{-4}
0.05	2.0×10^{-3}	3.4×10^{-3}	7.3×10^{-3}	8.5×10^{3}	0.86	1.1×10^{-3}	3.0×10^{-4}
0.1	2.2×10^{-3}	3.6×10^{-3}	7.4×10^{-3}	9.0×10^{3}	0.82	1.1×10^{-3}	3.5×10^{-4}
0.3	2.6×10^{-3}	3.1×10^{-3}	7.2×10^{-3}	7.8×10^{3}	0.94	1.3×10^{-3}	3.3×10^{-4}
0.5	3.8×10^{-3}	2.5×10^{-3}	7.3×10^{-3}	6.3×10^{3}	1.4	1.6×10^{-3}	3.9×10^{-4}
0.8	3.6×10^{-3}	2.9×10^{-3}	7.2×10^{-3}	7.2×10^{3}	1.0	1.9×10^{-3}	3.8×10^{-4}
1	5.0×10^{-3}	2.2×10^{-3}	7.5×10^{-3}	5.5×10^{3}	1.4	2.0×10^{-3}	4.0×10^{-4}
1.5	5.0×10^{-3}	2.3×10^{-3}	7.3×10^{-3}	5.7×10^{3}	1.3	2.2×10^{-3}	3.9×10^{-4}
2	6.6×10^{-3}	1.8×10^{-3}	8.1×10^{-3}	4.4×10^{3}	1.8	2.3×10^{-3}	3.9×10^{-4}
3	8.0×10^{-3}	1.5×10^{-3}	7.9×10^{-3}	3.7×10^{3}	2.1	2.5×10^{-3}	4.0×10^{-4}
4	8.0×10^{-3}	1.6×10^{-3}	8.0×10^{-3}	4.0×10^{3}	2.0	2.6×10^{-3}	3.9×10^{-4}

[a]The estimated standard deviation is within ±10% for each parameter.

($[\underline{P_t}]$) bound to the sensor surface and is insensitive to the subsequent steps following the initial binding to form $\underline{PG}$:

$$[\underline{P_t}] = [\underline{P^*}] + [\underline{PG}] + [\underline{PG_2}] + [\underline{PG_3}]) \quad (2)$$

As detailed in Supporting Information, under the steady-state approximation for P^*, the initial time profile of bound protein concentration is given by (see Supporting Information):

$$[\underline{P_t}] \approx \alpha[1 - \exp(-\beta t)] \quad (3)$$

The two coefficients are

$$\alpha = \frac{k_1}{k_{-1}}\frac{k_2}{k_{-2}}[P]_0[\underline{G}]_0 = K_1K_2[P]_0[\underline{G}]_0 \quad (4)$$

$$\beta = \frac{k_{-2}}{1 + [\underline{G}]_0 k_2/k_{-1}} \quad (5)$$

where K_1 (= k_1/k_{-1}) and K_2 (=k_2/k_{-2}) are the equilibrium constants for the two steps in eq 1. In this model, the kinetic profile depends explicitly on the precursor state. The proportionality constant, α, is a product of the two equilibrium constants and the starting concentrations of the protein in the solution and the glycan receptor on the membrane surface. A change in the membrane surface environment changes the equilibrium constant of the precursor state (K_1) and, thus, proportionally varies the formation rate of protein−glycan complexes.

The red curves in Figure 2A show fits of the initial kinetic profiles to eq 3, with the resulting kinetic parameters summarized in Table 1 and Figure 3A. We observe that α is increased 6 folds as the concentration of ϕ-OEG-lipid, denoted θ, is increased from 0 to 4%. A smaller change is observed in β, which decreases by 2.4 folds when ϕ-OEG-lipid is increased from 0 to 4%. These results can be easily understood from the precursor mechanism. The nonspecific adsorption of protein molecules is known to be more favorable on hydrophobic surfaces.[22] By increasing the concentration of the hydrophobic ϕ-OEG-lipid, the membrane surface becomes more attractive for the transient adsorption of weakly bound HA proteins and thus increases the equilibrium constant K_1 for the formation of the precursor state. Equation 4 predicts that an increase in K_1 corresponds proportionally to a larger value of α. As shown in eq 4, stronger binding in the precursor state (at higher ϕ-OEG-lipid concentration) can also be described by a smaller desorption rate constant k_{-1} and, thus, a decreased value of β (eq 5).

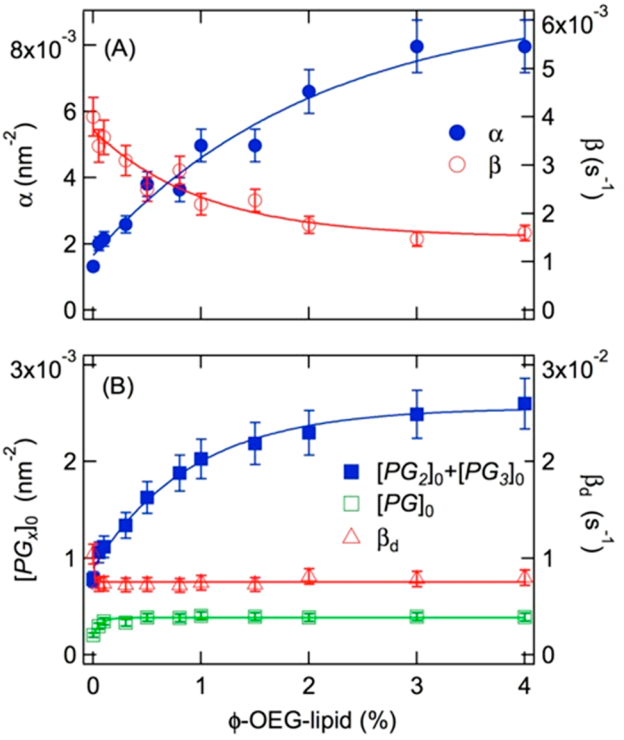

Figure 3. Kinetic parameters obtained from fits to (A) association (eq 3) and (B) dissociation (eq 6) parts of the SPR profiles in Figure 2A.

We now analyze dissociation kinetics from eq 1. For $t \geq 420$ s in Figure 2A, the protein solution is switched to washing buffer and $[P] = 0$. As detailed in the Supporting Information, the kinetic equations cannot be solved analytically and require numerical simulation. However, we can obtain an approximate solution at the short time limit, assuming that the initial dissociation from the membrane surface is dominated by that of the monovalent PG, with the concentrations of multivalent PG_2 and PG_3 remain nearly constant. This assumption is justified as the equilibrium constants of multivalent interactions are many orders of magnitude higher than the corresponding monovalent interaction. We further assume that the membrane surface concentration of free glycan receptor can be approximated as a constant, $[\underline{G'}]$, at the short time limit. The initial time profile of the surface bound protein concentration under these approximations is given by

dx.doi.org/10.1021/cb5004114 | ACS Chem. Biol. 2014, 9, 1877−1884

$$[\underline{P}_t] \approx [\underline{PG}]_0 \cdot \exp(-\beta' \cdot t') + [\underline{PG}_2]_0 + [\underline{PG}_3]_0) \quad (6)$$

where $[\underline{PG}]_0$ is the bound monovalent HA protein−glycan receptor complex at the time of washing buffer injection ($t' = 0$). $[\underline{PG}_2]_0$ and $[\underline{PG}_3]_0$ are the concentrations of bound multivalent HA protein−glycan receptor complex that are approximated as constants. β_d is given by

$$\beta = \frac{k_{-2}}{1 + [\underline{G}']k_2/k_{-1}} \quad (7)$$

The green curves in Figure 2A show fits of the initial dissociation profiles to eq 6, with resulting parameters summarized in Table 1 and Figure 3B. With increasing ϕ-OEG-lipid concentration, there is little change to β_d and $[\underline{PG}]_0$. The most important change is in $[\underline{PG}_x]_0 = [\underline{PG}_2]_0 + [\underline{PG}_3]_0$, which increases by three folds when the ϕ-OEG-lipid concentration is increased from 0 to 4%. We conclude that enhancing the binding of precursor protein molecules on the membrane surface leads predominantly to an increase in the concentration of multivalent $\underline{PG}_x$ ($x = 2, 3$) species.

To further understand the above precursor mechanism, we now compare this to the conventional protein-receptor binding model in which the formation of the complex occurs in a single step:

$$P + \underline{G} \underset{k_d}{\overset{k_a}{\rightleftharpoons}} \underline{PG} \quad (8)$$

where k_a and k_d are the association and dissociation constants, respectively. Further steps in the multivalent binding process to form $\underline{PG}_2$ and $\underline{PG}_3$ are identical to steps iii and iv in eq 1; as discussed earlier, these steps are not resolved in an SPR measurement. At the initial stage of binding, we apply the short time approximation and the time evolution of adsorbed protein signal is given by (see Supporting Information):

$$[\underline{P}_t] \approx [\underline{G}]_0[1 - \exp(-k_a[P]t)] \quad (9)$$

where $[P]$ (=0.4 μM) is the solution concentration of HA protein molecules; $[\underline{G}]_0$ is the starting concentration of glycan receptor, **33**-ϕ-OEG-lipid, in the supported lipid bilayer. Given the fraction (=0.8%) of **33**-ϕ-OEG-lipid in the SLB, and the lipid density (= 0.5 nm^{-2}) of the SLB,[38] we obtained $[\underline{G}]_0 = 1.6 \times 10^{-2}$ nm^{-2}.

Equation 9 is equivalent to eq 3, with $\alpha = [\underline{G}]_0$ and $\beta = k_a[P]$. This model is in clear contradiction to the fitting results in Table 1 for two reasons: (1) For all the SLBs probed in Figure 2A, the receptor (**33**) concentration is fixed at $[\underline{G}]_0 = 1.6 \times 10^{-2}$ nm^{-2}, but the fitting results show $[\underline{G}]_0$ (=α) increasing from 1.3×10^{-3} nm^{-2} to 8.0×10^{-3} nm^{-2} when ϕ-OEG-lipid increases from 0 to 3−4%; (2) with increasing secondary lipid (ϕ-OEG-lipid) in the SLB, the association constant k_a (=β/$[P]$) actually decreases, in contradiction to the observed increase in HA protein binding.

Further evidence against the direct association/dissociation model in eq 8 comes from analysis of dissociation rates and the equilibrium constant, $K_D = k_d/k_a$. Using the short-time limit approximation, the initial dissociation process from the direct mechanism in eq 8 can also be described by eq 6, with $\beta' = k_d$ (see Supporting Information). There is little change to k_d or K_D when the secondary ϕ-OEG-lipid concentration is increased from 0 to 3−4% in the SLB with fixed receptor (**33**-ϕ-OEG-lipid) concentration. Thus, the enhancement of HA protein binding to receptor **33**-ϕ-OEG-lipid in the SLB by the addition of ϕ-OEG-lipid, which by itself does not show any binding for HA (Supporting Information Figure S3), cannot be attributed to increased interaction between HA and the glycan receptor **33**. Rather, it is a kinetic effort in the precursor-mediated mechanism. Note that, within the inappropriate model of direct binding between solution HA protein and membrane surface glycan, the kinetic parameters (k_a and k_d) and dissociation equilibrium constant (K_D) obtained here (Table 1) are similar to numbers reported by Narla and Sun for the binding of HA from H5N1 to α2-3 linked sialic acids immobilized on the surface of SPR sensors.[27] However, our K_D values for the specific H5N1 HA/**33** interaction are more than 1 order of magnitude higher than that reported by Gaunitz et al.[26] and 4 orders of magnitude higher than those reported by Hidari et al.[28] for other HA/α2-3 linked sialic acid combinations, again pointing to the sensitivity of HA binding to the specific glycan linkages.

To understand how the membrane surface environment affects the precursor state and, thus, the specific binding of HA to **33**-ϕ-OEG-lipid, we show in Figure 4 SLB microarray results

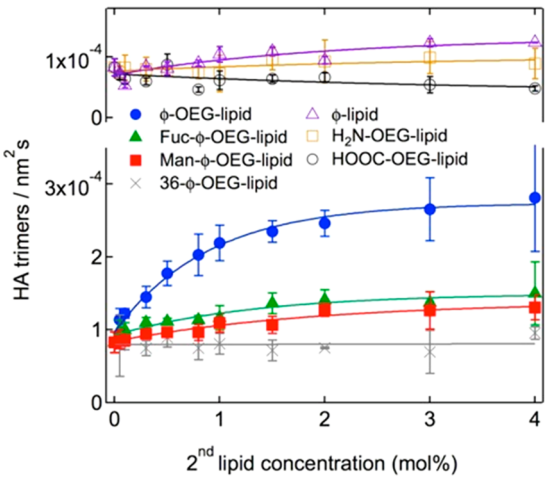

Figure 4. Initial rate of HA trimers (per nm^2, per second), obtained from the SPR responses for **33**-ϕ-OEG-lipid (0.8%) in the presence of varying concentrations of a second functional lipid (0−4%) in the SLB array. The different symbols represent different functional lipids as shown in the legend. The lines are exponential fits that serve as guides to the eye.

of **33**-ϕ-OEG-lipid (0.8%) in the presence of seven different secondary lipids with varying concentrations (0−4%). Here, the y-axis is the initial rate of HA binding on the membrane surface. These results provide microscopic insight into the precursor mechanism.

We first compare ϕ-OEG-lipid with ϕ-lipid. With increasing concentration of secondary lipid from 0 to 4%, ϕ-OEG-lipid increases bound HA density by 3.5 fold, but ϕ-lipid only increases that by 1.2 fold. Both secondary lipid molecules contain the ϕ hydrophobic functional group. The difference is height on the membrane surface: the ϕ-lipid is shorter than ϕ-OEG-lipid by the OEG linker (~2 nm). In the case of ϕ-OEG-lipid (blue solid circles), the precursor HA on ϕ-OEG-lipid is at a similar height from the membrane surface as the glycan receptor **33**, which is also spaced by the OEG linker. In comparison, the precursor HA on ϕ-lipid (purple open triangles) is lower than the glycan receptor by ~2 nm. These results suggest a *geometric barrier* for transiently bound HA

dx.doi.org/10.1021/cb5004114 | ACS Chem. Biol. 2014, 9, 1877−1884

molecules in the precursor state to interact specifically with the glycan receptor.

For other secondary lipids with functional group at similar heights from the membrane surface as the specific glycan receptor (**33**), we find enhancement or inhibition of HA binding, depending on the nature of the functionality. As the secondary lipid concentration is increased from 0 to 4%, mannose (solid red squares) and fucose (solid green triangles) show enhancements up to 1.6 and 1.8 fold, respectively; these glycosylated lipids are less hydrophobic than ϕ-OEG-lipid and are less effective in promoting the precursor state. The trisaccharide **36** with α2-6 linkage (gray crosses) and the -NH_2 group (yellow open squares) exhibit no enhancement, but the −COOH acid group (black open circles) decreases HA binding by up to 32% at 4% functional lipid concentration. These functionalities are hydrophilic and do not appreciably affect precursor binding.

Conclusions. The binding of glycan binding proteins to glycan receptors on cell membranes is fundamentally a kinetic process. Our findings reveal that this kinetic process is determined not only by the specific interaction within the binding pocket (and secondary interactions outside the pocket)[12] but also by weak and transient interactions in the precursor states. In the model system probed here, both HAs on virus surfaces and glycan receptors on cell membranes are present in complex and heterogeneous environments. While these local environments may have minimal effect on the specific binding between HAs and their glycan receptors, they can drastically affect the precursor state and, thus, the overall binding kinetics. Previous studies on influenza viruses, particularly the potential danger of avian influenza becoming transmittable in human, have mainly asked questions at the genetic level, e.g., how antigenic drifts, antigenic shifts, and specific mutation in the laboratory changes the HA binding specificity. A major challenge with the genetic approach is that our knowledge seems to be confined to quantum steps: we know a particular strain becomes transmittable in human only after the fact. We do not know *a priori* if certain genetic changes are increasing the affinity of a particular influenza A HA toward human host cells, that is, the continuum before the quantum step of human outbreak or pandemic. In view of the findings present here, we present the following hypotheses: (i) the quantized switching of influenza A virus HA affinity may be assisted by more gradual enhancement in precursor interaction on the host cell membrane surface; (ii) differences in cell surface environment in enhancing or inhibiting the nonspecific precursor interaction may partially account for individual variability to influenza A virus infection; (iii) disruption of the precursor state may be used as a strategy in the development of inhibitor or treatment of influenza A virus infection; (iv) the enhancement of weak interactions in the precursor state may be used as one of the "predictors" or "warning signals" for the potential danger of a particular virus stain. While we are far from being able to verify these hypotheses, we hope the potential importance of these hypotheses will motivate a new direction on influenza A virus research. The precursor mediate mechanism is of general significance to the understanding of a wide range of biological processes on membrane surfaces.

METHODS

See Supporting Information for methods.

ASSOCIATED CONTENT

Supporting Information

Experimental details and results from control experiments. This material is available free of charge *via* the Internet at http://pubs.acs.org/.

AUTHOR INFORMATION

Corresponding Authors

*Email: xyzhu@columbia.edu.
*Email: athena@microsurfacesinc.com.
*Email: h.w.liu@cm.utexas.edu.

Present Address

[‖]Huazhong University of Science and Technology, School of Chemistry and Chemical Engineering, Wuhan, China 430074

Notes

The authors declare the following competing financial interest(s): MicroSurfaces, Inc., a for-profit private company, is funded by an National Institutes of Health (NIH) SBIR-II grant to develop the membrane microarray used in the present study.

ACKNOWLEDGMENTS

All SPR measurements, as well as the synthesis of azide-mannose, azide-fucose, and ammine-functionalized triglycan, were supported by National Science Foundation grant CH1312646 awarded to Columbia University with a subcontract to the University of Texas at Austin. The development and fabrication of supported lipid bilayer microarray and the synthesis of glycol−lipid conjugates and functional lipid molecules were supported by an SBIR phase-II grant from National Institute of Health (2R44AI077161-02A1) awarded to MicroSurfaces, Inc. All azide-tagged trisaccharides were generously supplied by Consortium for Functional Glycomics. We thank M. Ruszczycky for a critical reading of this manuscript.

REFERENCES

(1) Mammen, M., Choi, S.-K., and Whitesides, G. M. (1998) Polyvalent interactions in biological systems: Implications for design and use of multivalent ligands and inhibitors. *Angew. Chem., Int. Ed. 37*, 2754−2794.
(2) Morens, D. M., Subbara, K., and Taubenberger, J. K. (2012) Engineering H5N1 avian influenza viruses to study human adaptation. *Nature 486*, 335−340.
(3) Fauci, A. S., and Collins, F. S. (2012) Benefits and risks of influenza research: Lessons learned. *Science 336*, 1522−1523.
(4) Herfst, S., et al. (2012) Aerosol transmission of avian influenza A/H5N1 virus between ferrets. *Science 336*, 1534−1541.
(5) Imai, M., et al. (2012) Experimental adaptation of an influenza H5 HA confers respiratory droplet transmission to a reassortant H5HA/H1N1 virus in ferrets. *Nature 486*, 420−428.
(6) Russell, C. A., et al. (2012) The potential for respiratory droplet-transmissible a/h5n1 influenza virus to evolve in a mammalian host. *Science 336*, 1541−1547.
(7) Garten, R. J., et al. (2009) Antigenic and genetic characteristics of swine-origin 2009 A(H1N1) influenza viruses circulating in humans. *Science 325*, 197−201.
(8) Gao, R., et al. (2013) Human infection with a novel avian-origin influenza A (H7N9) virus. *N. Engl. J. Med. 368*, 1888−1897.
(9) Skehel, J. J., and Wiley, D. C. (2000) Receptor binding and membrane fusion in virus entry: The influenza hemagglutinin. *Annu. Rev. Biochem. 69*, 531−569.
(10) Medina, R. A., and García-Sastre, A. (2011) Influenza A viruses: New research developments. *Nat. Rev. Microbiol. 9*, 590−603.

(11) Sauter, N. K., et al. (1992) Binding of influenza virus hemagglutinin to analogs of its cell-surface receptor, sialic acid: Analysis by proton nuclear magnetic resonance spectroscopy and X-ray crystallography. *Biochemistry 31*, 9609−9621.
(12) Stevens, J., Blixt, O., Tumpey, T. M., Taubenberger, J. K., Paulson, J. C., and Wilson, I. A. (2006) Structure and receptor specificity of the hemagglutinin from an H5N1 influenza virus. *Science 312*, 404−410.
(13) Connor, R. J., Kawaoka, Y., Webster, R. G., and Paulson, J. C. (1994) Receptor specificity in human, avian, and equine H2 and H3 influenza virus isolates. *Virology 205*, 17−23.
(14) Stevens, J., Blixt, O., Paulson, J. C., and Wilson, I. A. (2006) Glycan microarray technologies: Tools to survey host specificity of influenza viruses. *Nat. Rev. Microbiol. 4*, 857−864.
(15) Shinya, K., Ebina, M., Yamada, S., Ono, M., Kasai, N., and Kawaoka, Y. (2006) Avian flu: Influenza virus receptors in the human airway. *Nature 440*, 435−436.
(16) Viswanathan, K., Chandrasekaran, A., Srinivasan, A., Raman, R., Sasisekharan, V., and Sasisekharan, R. (2010) Glycans as receptors for influenza pathogenesis. *Glycoconj. J. 27*, 561−570.
(17) Liao, H. Y., Hsu, C. H., Wang, S. C., Liang, C. H., Yen, H. Y., Su, C. Y., Chen, C. H., Jan, J. T., Ren, C. T., Chen, C. H., Cheng, T. J. R., Wu, C. Y., and Wong, C. H. (2010) Differential receptor binding affinities of influenza hemagglutinins on glycan arrays. *J. Am. Chem. Soc. 132*, 14849−14856.
(18) Chandrasekaran, A., Srinivasan, A., Raman, R., Viswanathan, K., Raguram, S., Tumpey, T. M., Sasisekharan, V., and Sasisekharan, R. (2008) Glycan topology determines human adaptation of avian H5N1 virus hemagglutinin. *Nat. Biotechnol. 26*, 107−113.
(19) Kisliuk, P. (1957) The sticking probabilities of gases chemisorbed on the surfaces of solids. *J. Phys. Chem. Solids 3*, 95−101.
(20) de Gennes, P. G. (1981) Polymer solutions near an interface. Adsorption and depletion layers. *Macromolecules 14*, 1637−1644.
(21) Stuart, M. A. C., and Fleer, G. J. (1996) Adsorbed polymer layers in nonequilibrium situations. *Annu. Rev. Mater. Sci. 26*, 463−500.
(22) Garland, A., Shen, L., and Zhu, X.-Y. (2012) Mobile precursor state mediated protein adsorption on solid surfaces. *Prog. Surf. Sci. 87*, 1−22.
(23) Shen, L., Adachi, T., Venden Bout, D. A., and Zhu, X.-Y. (2012) A mobile precursor determines amyloid-β peptide fibril formation at the liquid−solid interface. *J. Am. Chem. Soc. 134*, 14172−14178.
(24) Schreiber, G. (2002) Kinetic studies of protein−protein interactions. *Curr. Opin. Struct. Biol. 12*, 41−47.
(25) Zhu, X.-Y., Holtz, B., Wang, Y., Wang, L.-X., Orndorff, P. E., and Guo, A. (2009) Quantitative glycomics from fluidic glycan microarrays. *J. Am. Chem. Soc. 131*, 13646−13650.
(26) Gaunitz, S., Liu, J., Nilsson, A., Karlsson, N., and Holgersson, J. (2014) Avian influenza H5 hemagglutinin binds with high avidity to sialic acid on different O-linked core structures on mucin-type fusion proteins. *Glycoconjugate J. 31*, 145−159.
(27) Narla, S. N., and Sun, X. L. (2012) Immobilized sialyloligomacroligand and its protein binding specificity. *Biomacromolecules 13*, 1675−1682.
(28) Hidari, K. I., Shimada, S., Suzuki, Y., and Suzuki, T. (2007) Binding kinetics of influenza viruses to sialic acid-containing carbohydrates. *Glycoconjugate J. 24*, 583−590.
(29) Watanabe, Y., Ibrahim, M. S., Suzuki, Y., and Ikuta, K. (2012) The changing nature of avian influenza A virus (H5N1). *Trends Microbiol. 20*, 11−20.
(30) Wei, C.-J., et al. (2008) Comparative efficacy of neutralizing antibodies elicited by recombinant hemagglutinin proteins from avian H5N1 influenza virus. *J. Virol. 82*, 6200−6208.
(31) Ruigrok, R. W. H., et al. (1988) Studies on the structure of the influenza virus haemagglutinin at the pH of mebrane fusion. *J. Gen. Virol. 69*, 2785−2795.
(32) Brian, A. A., and McConnell, H. M. (1984) Allogeneic stimulation of cytotoxic T cells by supported planar membranes. *Proc. Natl. Acad. Sci. U.S.A 81*, 6159−6163.
(33) Deng, Y., Wang, Y., Holtz, B., Li, J.-Y., Traaseth, N., Veglia, G., Stottrup, B., Pei, D., Elde, R., Guo, A., and Zhu, X.-Y. (2008) Fluidic and air-stable supported lipid bilayer and cell-mimicking microarray. *J. Am. Chem. Soc. 130*, 6267−6271.
(34) Mossman, K., and Groves, J. T. (2007) Micropatterned supported membranes as tools for quantitative studies of the immunological synapse. *Chem. Soc. Rev. 36*, 46−54.
(35) http://www.functionalglycomics.org/static/consortium/consortium.shtml.
(36) Koo, H., et al. (2012) Bioorthogonal copper-free click chemistry *in vivo* for tumor-targeted delivery of nanoparticles. *Angew. Chem., Int. Ed. 51*, 11836−11840.
(37) Boraston, A. B., Bolam, D., Gilbert, H., and Davies, G. J. (2004) Carbohydrate-binding modules: Fine-tuning polysaccharide recognition. *Biochem. J. 382*, 769−781.
(38) Goertz, M., Stottrup, B. L., Houston, J. E., and Zhu, X.-Y. (2009) Nanomechanical contrasts of gel versus fluid phase supported lipid bilayers. *J. Phys. Chem. B 113*, 9335−9339.